
Consistent Dropout for Policy Gradient Reinforcement Learning

Matthew Hausknecht¹ Nolan Wagener²

Abstract

Dropout has long been a staple of supervised learning, but is rarely used in reinforcement learning. We analyze why naïve application of dropout is problematic for policy-gradient learning algorithms and introduce *consistent dropout*, a simple technique to address this instability. We demonstrate consistent dropout enables stable training with A2C and PPO in both continuous and discrete action environments across a wide range of dropout probabilities. Finally, we show that consistent dropout enables the online training of complex architectures such as GPT without needing to disable the model’s native dropout.

1. Introduction

Dropout, the practice of randomly zeroing a fraction of unit activations at select neural network layers, is an established technique for regularizing neural network learning and reducing overfitting (Srivastava et al., 2014). However, in the field of reinforcement learning, dropout is rarely applied. Consider the large body of work without dropout, including high-profile projects like AlphaGo (Silver et al., 2016), AlphaStar (Vinyals et al., 2019), and OpenAI Five (Berner et al., 2019) – none of which mention dropout. Even models that are commonly supervised-trained with dropout, such as Transformers (Vaswani et al., 2017), disable dropout entirely when repurposed for reinforcement learning (Parisotto et al., 2019; Loynd et al., 2020). This trend is reinforced by our open source tools: Surveying six popular open source RL frameworks¹, we found none that supported dropout.

We contend that the naïve application of dropout in reinforcement learning can be detrimental to learning performance. To test this hypothesis, we added dropout layers to

the policy networks of A2C and PPO agents in three RL frameworks: RLlib (Liang et al., 2017), Stable-Baselines3 (Raffin et al., 2019), and Tianshou (Weng et al., 2020). Agents were then trained on the MuJoCo Half-Cheetah-v3 continuous control environment using the hyperparameters recommended by their respective codebases. To summarize results in Appendix B, Tianshou’s A2C experienced large negative returns (e.g., -10^7) in five of sixteen runs, and all sixteen PPO runs prematurely terminated due to NaN values. Similarly, RLlib experienced instability in five of six A2C runs and two of six PPO runs. Stable-Baselines3, on the other hand, completed all runs without error, though we found that A2C experienced large policy loss magnitudes on seven of twelve runs and PPO declined in performance by 21% on average with dropout. Thus, we conclude that instability stemming from naïve application of dropout is not an artifact of a single implementation or codebase but instead affects to various degrees all of the tested frameworks.²

To better understand *why* dropout is problematic, Section 4 shows the instability stems from different dropout masks being applied to the same observations during rollouts and updates. This mismatch leads to policy collapse for A2C and reduced performance for PPO. Furthermore, we show that more complex networks such as GPT (Radford et al., 2019) suffer more acutely than MLPs from the instabilities introduced by naïve application of dropout. To correct this instability, Section 5 introduces *consistent dropout*, a simple and mathematically sound technique that consists of saving the random dropout masks generated during rollouts and reapplying the same masks during updates. Experimental results in Section 6 show this technique stabilizes learning for both A2C and PPO on discrete and continuous environments across a spectrum of dropout probabilities. We also show this technique allows for GPT to be trained online without needing to disable dropout.

The contributions of this paper are: 1) Demonstrate that naïve application of dropout creates instability for policy gradient methods across a variety of open-source RL frameworks, algorithms, and environments. 2) Analyze the source of instability and introduce a simple method of saving and

¹Microsoft Research ²Institute for Robotics and Intelligent Machines, Georgia Institute of Technology. Correspondence to: Matthew Hausknecht <matthew.hausknecht@gmail.com>, Nolan Wagener <nolan.wagener@gatech.edu>.

¹Surveyed frameworks were Dopamine (Castro et al., 2018), RLlib (Liang et al., 2017), OpenAI Baselines (Dhariwal et al., 2017), Tianshou (Weng et al., 2020), Stable-Baselines3 (Raffin et al., 2019), and rlypt (Stooke & Abbeel, 2019).

²Notably, the use of Tanh nonlinearities in policy networks reduced instability compared to ReLU. Although we did not perform a detailed investigation, we suspect this relates to Tanh bounding the network outputs.

reapplying dropout masks to stabilize training. 3) Demonstrate stable online RL training of GPT with dropout.

2. Related Work

Farebrother et al. (2018) investigated dropout as a regularization technique for the DQN learning agent (Mnih et al., 2015) on Atari environments. Their findings indicate that moderate levels of dropout ($p = 0.1$), paired with ℓ_2 regularization improved zero-shot generalization on variants of the training environment. However, the authors note that dropout slowed the training performance and typically required more training iterations to compete with the unregularized baseline.

Similarly, Cobbe et al. (2018) examined the effects of dropout and ℓ_2 regularization on the Procgen benchmark (Cobbe et al., 2019). Using the PPO algorithm, they found both ℓ_2 regularization and moderate levels of dropout ($p = 0.1$) aided generalization to held-out test environments, but also slightly reduced performance on training environments.³

Dropout has been successfully applied in sequential decision making settings when training is based on offline RL or imitation learning. Examples such as the Decision Transformer (Chen et al., 2021) and Trajectory Transformer (Janner et al., 2021) show that transformer models are capable of learning high quality policies from offline expert data. In this work we show how such models can be additionally trained with online RL, potentially enabling a paradigm of offline pretraining followed by online finetuning.

3. Preliminaries

We consider an infinite-horizon Markov decision process (MDP) defined as the tuple $\mathcal{M} = (\mathcal{S}, \mathcal{A}, p, R, \gamma)$, where \mathcal{S} is the state space, \mathcal{A} is the action space, $p(s'|s, a)$ is the transition kernel, $R(s, a)$ is the reward function, and γ is the discount factor. Let $\pi_\theta(a|s)$ be a stochastic policy parameterized by some vector θ . Given some start state distribution $d_0(s_0)$, the policy and transition kernel induce a trajectory distribution $\rho^{\pi_\theta}(\tau)$, where $\tau = (s_0, a_0, s_1, a_1, \dots)$. Our goal is to find a parameter setting that maximizes the expected sum of discounted rewards in the MDP:

$$\max_{\theta} J(\theta) = \mathbb{E}_{\rho^{\pi_\theta}(\tau)} \left[\sum_{t=0}^{\infty} \gamma^t R(s_t, a_t) \right].$$

We define the value function $V^{\pi_\theta}(s)$ and state-action value

³Inspection of the [CoinRun codebase](#) indicates Cobbe et al. implemented a variant of consistent dropout, but it is neither mentioned in the paper nor analyzed.

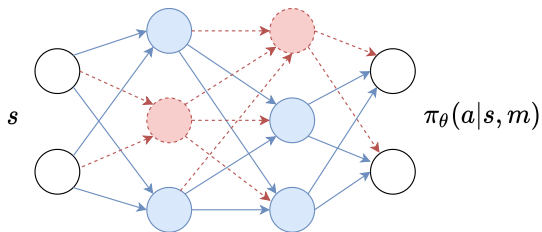


Figure 1. An example of a policy after a dropout mask m has been sampled. The neurons in red have their activations zeroed out.

function $Q^{\pi_\theta}(s, a)$ as:

$$V^{\pi_\theta}(s) = \mathbb{E}_{\rho^{\pi_\theta}(\tau)} \left[\sum_{t=0}^{\infty} \gamma^t R(s_t, a_t) \mid s_0 = s \right]$$

$$Q^{\pi_\theta}(s, a) = \mathbb{E}_{\rho^{\pi_\theta}(\tau)} \left[\sum_{t=0}^{\infty} \gamma^t R(s_t, a_t) \mid s_0 = s, a_0 = a \right]$$

and furthermore define the advantage function $A^{\pi_\theta}(s, a) = Q^{\pi_\theta}(s, a) - V^{\pi_\theta}(s)$.

Let $d_t^{\pi_\theta}(s)$ be the state distribution induced by running π_θ in \mathcal{M} for t time steps from the initial state distribution d_0 . Defining the state visitation $d^{\pi_\theta}(s) = (1 - \gamma) \sum_{t=0}^{\infty} \gamma^t d_t^{\pi_\theta}(s)$, it can be shown (Sutton et al., 2000) that the policy gradient has the form

$$\nabla J(\theta) = \mathbb{E}_{d^{\pi_\theta}(s)} \mathbb{E}_{\pi_\theta(a|s)} [A^{\pi_\theta}(s, a) \nabla_{\theta} \log \pi_\theta(a|s)]. \quad (1)$$

Practical implementations of policy gradient algorithms roll out π_θ and collect state-action-reward triplets (s, a, r) into a buffer \mathcal{D} . After learning an approximate advantage function $\hat{A}(s, a)$ (e.g., through generalized advantage estimation (Schulman et al., 2016)), they form the loss function

$$L_{PG}(\theta) = -\mathbb{E}_{(s,a) \sim \mathcal{D}} [\hat{A}(s, a) \log \pi_\theta(a|s)] \quad (2)$$

and subsequently perform a gradient descent step.

4. Why Dropout Disrupts Policy Gradient

We now assume that π_θ is a multi-layer neural network where there is a subset of neurons wherein each activation is zeroed out with some probability, as shown in Fig. 1. Letting m be the resulting dropout mask, our stochastic policy has the form $\pi_\theta(a|s) = \sum_m p(m) \pi_\theta(a|s, m)$, where $p(m)$ is the probability function of the mask. In practice, dropout is treated as an unobserved internal process of the network, so that we observe a noisy estimator of $\pi_\theta(a|s)$.

Due to this practice, at rollout time, we sample some dropout mask \hat{m} at a given state s and then sample an action from $\pi_\theta(a|s, \hat{m})$ to apply in the MDP. At update time, we sample

Table 1. Forward passes over the same state with different dropout masks change output actions and reduce the log probabilities: Let a^0 and a^1 be the most likely (i.e., mode) actions from two forward passes on the same state s using random dropout masks m^0 and m^1 , respectively. For continuous actions, $d(a^0, a^1)$ is the absolute difference $|a^0 - a^1|$. For discrete actions, $d(a^0, a^1)$ indicates the frequency of disagreement $\mathbb{P}[a^0 \neq a^1]$. Higher levels of dropout result in greater differences in actions as well as lower log probabilities. This effect is more pronounced in GPT, in which a dropout probability of 0.1 is approximately equivalent to an MLP with dropout of 0.75.

NET	DROPOUT	$d(a^0, a^1)$	$\log \pi_\theta(a^0 s, m^1)$
3-LAYER	0	0 ± 0	-0.83 ± 0.00
MLP w/	0.1	0.04 ± 0.03	-0.84 ± 0.01
4 CONTINUOUS	0.25	0.06 ± 0.05	-0.86 ± 0.02
ACTIONS	0.5	0.12 ± 0.09	-0.90 ± 0.07
	0.75	0.23 ± 0.25	-1.13 ± 0.38
	0.9	0.63 ± 0.65	-6.36 ± 7.04
4-LAYER	0	0 ± 0	-0.83 ± 0.00
GPT w/	0.1	0.26 ± 0.20	-1.14 ± 0.33
4 CONTINUOUS	0.25	0.41 ± 0.32	-1.57 ± 0.77
ACTIONS	0.5	0.52 ± 0.40	-2.01 ± 1.21
	0.75	0.62 ± 0.47	-2.47 ± 1.63
	0.9	0.64 ± 0.49	-2.64 ± 1.80
3-LAYER	0	0 ± 0	-1.31 ± 0.03
MLP w/	0.1	0.18 ± 0.39	-1.35 ± 0.04
4 DISCRETE	0.25	0.51 ± 0.50	-1.34 ± 0.05
ACTIONS	0.5	0.60 ± 0.48	-1.34 ± 0.10
	0.75	0.71 ± 0.47	-1.39 ± 0.21
	0.9	0.75 ± 0.43	-1.51 ± 0.58

a new dropout mask when querying the policy for its log-probability. This results in a modified loss function for policy optimization:

$$\tilde{L}_{PG}(\theta) = -\mathbb{E}_{(s,a) \sim \mathcal{D}} \mathbb{E}_{p(m)} [\hat{A}(s, a) \log \pi_\theta(a|s, m)].$$

The use of different dropout masks for the same state s at rollout time versus update time can lead to vastly different action probabilities. For A2C, this manifests in $\pi_\theta(a|s)$ being close to zero and $\log \pi_\theta(a|s)$ approaching negative infinity. At this point, updates become unstable as policy loss and gradient magnitudes explode. In practice, gradient clipping can keep training numerically stable, but learning performance still suffers due to the gradient estimator having high variance. Table 1 demonstrates how the application of different dropout masks can change the outputs and lower the log probabilities of actions in an untrained, newly initialized network. These effects only become more pronounced over the course of training.

4.1. Dropout and PPO

PPO (Schulman et al., 2017) optimizes a clipped objective that ensures the deviation of the current policy π_θ from the

rollout policy $\pi_{\theta_{\text{old}}}$ is small:

$$L_{PPO}(\theta) = -\mathbb{E}_{\mathcal{D}} [\min\{r(s, a, \theta) \hat{A}(s, a), \text{clip}(r(s, a, \theta), 1 - \epsilon, 1 + \epsilon) \hat{A}(s, a)\}],$$

where $r(s, a, \theta) = \frac{\pi_\theta(a|s)}{\pi_{\theta_{\text{old}}}(a|s)}$ is the ratio of the action probabilities under the new and old policies, respectively, and ϵ is a small constant which determines how far the policy is allowed to diverge from the old policy. In addition to this clipped objective, PPO also has the option to stop taking gradient steps if the KL divergence between the new and old policies grows past a threshold. This early stopping mechanism can help ensure monotonic policy improvement by preventing gradient updates from extrapolating too far in any direction.

Adding dropout to the policy network increases the variance in the ratio of action probabilities r . The PPO objective clips this variance and prevents policy loss $L_{PPO}(\theta)$ from exploding. When using an early stopping threshold, we find that increased variance in r will often trigger immediate early stopping, preventing any updates from taking place. To preface our results, without early stopping we observe stable learning but notably reduced performance.

5. Policy Gradient with Dropout

We now present two methods to correctly compute the policy gradient in Eq. (1) in the presence of dropout.

5.1. Dropout-Marginalized Gradient

This method gives the correct policy gradient by marginalizing over possible dropout masks that are randomly sampled at update time: For some $s \in \mathcal{S}$ and $a \in \mathcal{A}$, the policy’s score function can be computed as:

$$\begin{aligned} \nabla_\theta \log \pi_\theta(a|s) &= \nabla_\theta \log \left(\sum_m p(m) \pi_\theta(a|s, m) \right) \\ &= \frac{\sum_m p(m) \pi_\theta(a|s, m) \nabla_\theta \log \pi_\theta(a|s, m)}{\sum_m p(m) \pi_\theta(a|s, m)} \\ &= \sum_m p(m|s, a, \theta) \nabla_\theta \log \pi_\theta(a|s, m). \end{aligned} \quad (3)$$

Thus, the score function is the expected score function of the dropout-conditioned policy under the posterior distribution of the dropout mask.

In this work, we use Eq. (3) to compute the score function. Since it is intractable to enumerate every dropout mask, we instead rely on sampling. For some $s \in \mathcal{S}$ and $a \in \mathcal{A}$, we sample N dropout masks m_1, \dots, m_N i.i.d. from $p(m)$.

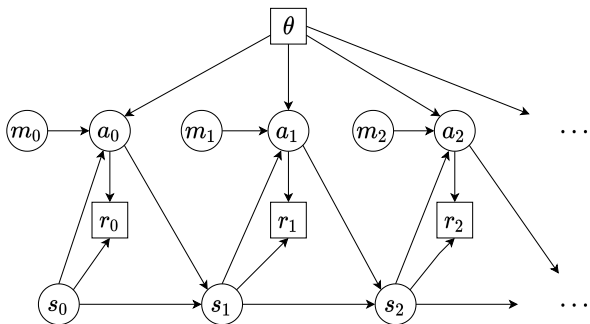


Figure 2. Stochastic computation graph (Schulman et al., 2015) of the MDP including the dropout mask m

For some mask m_n , we compute the weight

$$w_n = \frac{p(m_n)\pi_\theta(a|s, m_n)}{\sum_{k=1}^N p(m_k)\pi_\theta(a|s, m_k)},$$

whereupon the score function can be estimated as:

$$\nabla_\theta \log \pi_\theta(a|s) \approx \sum_{n=1}^N w_n \nabla_\theta \log \pi_\theta(a|s, m_n).$$

We note that the weights approximate the mask posterior, i.e., $w_n \approx p(m_n|s, a, \theta)$. The estimated score function can then be used to compute the policy gradient in Eq. (1).

This method has the advantage of not needing to store the dropout mask m when rolling out the policy π_θ , but the multiple samples required to compute the approximate mask posterior can lead to computational overhead for larger networks.

5.2. Dropout-Conditioned Gradient

Consider the modified MDP (Fig. 2) in which the policy outputs both the action and the dropout mask (a, m) , so that the stochastic policy is now $\pi_\theta(a, m|s) = p(m)\pi_\theta(a|s, m)$. This MDP is equivalent to the original since neither the dynamics nor the reward are modified, i.e., $p(s'|s, a, m) = p(s'|s, a)$ and $R(s, a, m) = R(s, a)$. As a consequence, the advantage function A^{π_θ} remains a function only of the state s and original action a .

Now, the score function of the policy is:

$$\begin{aligned} \nabla_\theta \log \pi_\theta(a, m|s) &= \nabla_\theta (\log p(m) + \log \pi_\theta(a|s, m)) \\ &= \nabla_\theta \log \pi_\theta(a|s, m) \end{aligned}$$

so that the resultant policy gradient is

$$\begin{aligned} \nabla J(\theta) &= \mathbb{E}_{d^{\pi_\theta}(s)} \mathbb{E}_{\pi_\theta(a, m|s)} [A^{\pi_\theta}(s, a) \nabla_\theta \log \pi_\theta(a, m|s)] \\ &= \mathbb{E}_{d^{\pi_\theta}(s)} \mathbb{E}_{\pi_\theta(a, m|s)} [A^{\pi_\theta}(s, a) \nabla_\theta \log \pi_\theta(a|s, m)]. \end{aligned}$$

Thus, we conclude that conditioning the policy on the same mask m that is sampled during rollouts results in

an unbiased policy gradient at update time. Finally, we note that while the derivations in the preceding sections are specialized to dropout, they can be easily extended to other networks that internally use stochasticity, such as Bayesian neural networks and hidden layers that rely on sampling.

5.3. Implementation

From an implementation perspective, due to the computational challenges of using the dropout-marginalized gradient (explored in Section 6.1), we focus on the dropout-conditioned gradient for the remainder of this work and refer to it as *consistent dropout*. At rollout time, for some state s , we sample a mask m and action a from $\pi_\theta(a, m|s)$, observe a reward r , and store the tuple (s, a, r, m) into a buffer \mathcal{D} . During subsequent updates, the saved masks can be reapplied with the corresponding states and actions. The resulting policy loss we optimize has the form:

$$L_{PG}(\theta) = -\mathbb{E}_{(s, a, m) \sim \mathcal{D}} [\hat{A}(s, a) \log \pi_\theta(a|s, m)].$$

This reuse of dropout masks ensures that any change in the policy network’s output is due to a change in the policy network’s weights, rather than a different dropout mask.

To facilitate easy storage and retrieval of masks, we design a custom dropout layer shown in Figure 3 that retains the most recent masks from the forward pass, where they can be easily stored and reapplied at update time. From a computational perspective, this approach is essentially just as fast as the original, but does require additional storage of dropout masks whose size and number vary based on the architecture of the policy net. However, by storing masks as binary arrays, we find they often take less space than states or actions. Finally, additional source code and examples showing the use of this consistent dropout layer may be found in the supplementary materials.

6. Experiments

In order to compare consistent and inconsistent dropout, we evaluate A2C and PPO on several popular continuous and discrete environments. In particular, the aim of our experiments is to empirically understand the effects of inconsistent dropout on policy gradient algorithms and to understand if consistent dropout stabilizes policy gradient learning.

6.1. Continuous-Action Environments

We conduct experiments on the Hopper, Walker2d, and Half-Cheetah MuJoCo tasks to compare the stability and performance of A2C and PPO when trained with consistent and inconsistent dropout probabilities of (0/0.1/0.25/0.5).

Results on Half-Cheetah are shown in Figure 5 and similar results from the other MuJoCo tasks may be found in Appendix C. Across all MuJoCo environments, we find

```

import torch
from torch import nn

class ConsistentDropout(nn.Module):
    """
    Consistent Dropout Layer uses masks provided in source and stores masks in sink.
    """
    def __init__(self, source, sink, p=0.5):
        super().__init__()
        self.source = source
        self.sink = sink
        self.p = p
        self.scale_factor = 1 / (1 - self.p)

    def forward(self, x):
        if self.training:
            if self.source:
                mask = self.source.pop(0)
            else:
                mask = torch.bernoulli(x.data.new(x.data.size()).fill_(1-self.p))
            self.sink.append(mask.bool())
            return x * mask * self.scale_factor
        else:
            return x

class ConsistentPolicyNet(nn.Module):
    def __init__(self, obs_size, action_size, hidden_size, dropout):
        super().__init__()
        self.source, self.sink = [], []
        self.policy_net = nn.Sequential(
            nn.Linear(obs_size, hidden_size),
            nn.ReLU(),
            ConsistentDropout(self.source, self.sink, p=dropout),
            nn.Linear(hidden_size, hidden_size),
            nn.ReLU(),
            ConsistentDropout(self.source, self.sink, p=dropout),
            nn.Linear(hidden_size, action_size)
        )

    def forward(self, obs, dropout_masks=None):
        if dropout_masks:
            self.source.extend(dropout_masks)
        action = self.policy_net(obs)
        masks = self.sink.copy()
        self.source.clear()
        self.sink.clear()
        return action, masks

```

Figure 3. Consistent Dropout Layer: PyTorch implementation of the consistent dropout layer and modifications needed to integrate into a policy network: The ConsistentDropout layer will retrieve and apply a dropout mask if provided in source and save the used dropout mask to sink. ConsistentPolicyNet demonstrates the integration of the ConsistentDropout layer into a policy network: Both source and sink are implemented using lists shared between all dropout layers in the network. In the forward pass, if dropout masks are provided they will be applied in correct order. Otherwise, random masks will be generated and returned. Returned masks can then be stored in the agent's replay memory and reapplied at update time.

Table 2. Relative Performance Under Dropout: Training performance relative to a baseline that does not use dropout. Across most environments, A2C with inconsistent dropout becomes unstable and achieves nearly zero performance. Consistent A2C (A2C-C) and Consistent PPO (PPO-C) achieve significantly more performance than their inconsistent counterparts on all MuJoCo environments. In Atari environments, PPO and PPO-C are much closer in relative performance with the trend favoring PPO-C.

DROP	A2C	A2C-C	PPO	PPO-C
HALFCHEETAH-V3				
0.1	0 ± 0	0.77 ± 0.03	0.61 ± 0.08	0.95 ± 0.07
0.25	0 ± 0	0.72 ± 0.09	0.21 ± 0.01	0.82 ± 0.12
0.5	0 ± 0	0.49 ± 0.03	0.07 ± 0.09	0.55 ± 0.11
HOPPER-V3				
0.1	0 ± 0	1.04 ± 0.06	1.08 ± 0.31	1.04 ± 0.2
0.25	0 ± 0	1.05 ± 0.03	0.79 ± 0.10	1.00 ± 0.21
0.5	0 ± 0	0.98 ± 0.05	0.31 ± 0.05	1.08 ± 0.34
WALKER2D-V3				
0.1	0 ± 0	0.90 ± 0.10	0.27 ± 0.05	0.91 ± 0.08
0.25	0 ± 0	0.96 ± 0.14	0.08 ± 0.01	0.55 ± 0.05
0.5	0 ± 0	0.50 ± 0.08	0.02 ± 0.00	0.40 ± 0.03
BEAMRIDER				
0.1	0.14 ± 0.10	0.48 ± 0.07	0.38 ± 0.04	0.70 ± 0.22
0.25	0.08 ± 0.06	0.43 ± 0.03	0.40 ± 0.07	0.51 ± 0.25
0.5	0.07 ± 0.10	0.23 ± 0.09	0.16 ± 0.02	0.17 ± 0.03
BREAKOUT				
0.1	0 ± 0	1.12 ± 0.63	0.64 ± 0.03	0.77 ± 0.04
0.25	0.01 ± 0	0.94 ± 0.13	0.56 ± 0.10	0.68 ± 0.08
0.5	0.01 ± 0	0.36 ± 0.13	0.53 ± 0.08	0.28 ± 0.03
SEQUEST				
0.1	1.56 ± 1.45	2.08 ± 0.53	1.13 ± 0.09	1.10 ± 0.25
0.25	0.34 ± 0.39	1.57 ± 0.34	0.99 ± 0.06	0.97 ± 0.07
0.5	1.5 ± 1.33	2.13 ± 0.89	1.01 ± 0.12	1.10 ± 0.32

that A2C is highly unstable for any level of inconsistent dropout. PPO is more robust to inconsistent dropout and often remains stable and performant at dropout of 0.1. However, dropout probabilities of 0.25 and 0.5 degrade PPO’s performance significantly.

On the other hand, as shown in Table 2, consistent dropout effectively stabilizes A2C and PPO across all MuJoCo environments and dropout levels. All levels of consistent dropout lead to stable learning, although dropout of 0.5 notably reduces performance for both algorithms.

In terms of absolute performance, baseline models without dropout perform slightly better on average than equivalent models trained with dropout. This finding reflects the intuition that when training and testing on the same environment, less regularization is likely beneficial.

We also experimented with a version of PPO that uses an estimate of the marginalized gradient in Eq. (3). As shown in Fig. 4, the large variance of the gradient estimate dominates the learning, even with 100 samples used for Eq. (3).

6.2. Discrete-Action Environments

We tested three discrete-action Atari environments (Beamrider, Breakout, and Seaquest), and as shown in Table 2 A2C

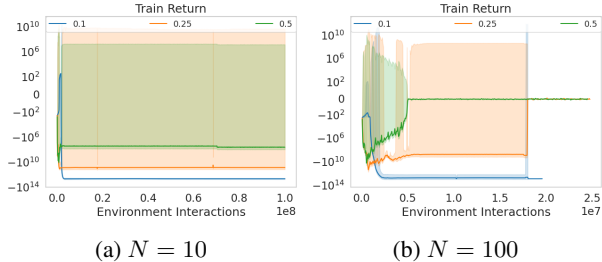


Figure 4. Marginalized Gradient: PPO training with marginalized gradients on HalfCheetah-v3. High variance gradient estimates lead to highly unstable learning dynamics.

is intolerant to any amount of inconsistent dropout. On the other hand, PPO often benefits from low-levels of inconsistent dropout (e.g., 0.1). We believe the source of this benefit stems from an increase in policy entropy. Nevertheless, inconsistent dropout triggers PPO’s KL divergence-based early stopping, which prevents updates from occurring and precludes any policy learning. Therefore, to facilitate training we disabled PPO’s early stopping and forced a set number of gradient steps to be performed at each update.

Consistent dropout leads to stable learning (Fig. 6), but we observed that policies can become overly confident in their actions, as evidenced by quickly growing action probabilities and shrinking policy entropy. Full Atari results may be found in Appendix D.

6.3. Stable GPT Training

Prior work on training transformer models with reinforcement learning disable dropout (Parisotto et al., 2019; Loynd et al., 2020). This is unsurprising as even small levels of dropout cause much larger changes to GPT’s outputs compared to similarly deep MLP networks (Table 1). As a result, PPO models trained with inconsistent dropout are unable to exceed random performance on Half-Cheetah. On the other hand, consistent dropout (Fig. 7) enables stable GPT training across all dropout probabilities. Extrapolating from this result, we believe consistent dropout is applicable to a variety of network architectures.

7. Evaluating with Dropout

Common practice for supervised learning is to disable dropout at evaluation time. However, it is unclear whether this practice would be beneficial for sequential decision making. To answer this question, we examined the effects of enabling or disabling dropout at evaluation time, and found a strong preference towards disabling dropout at evaluation time (Fig. 8). Specifically we observe a 2% improvement on average in final evaluation score when disabling dropout at evaluation time for the $p = 0.1$ models, a 17% improvement for the $p = 0.25$ models, and a 46% improvement in

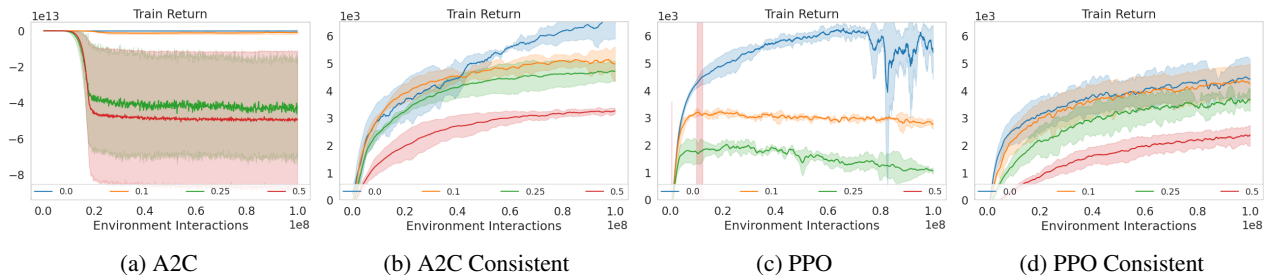


Figure 5. MuJoCo-HalfCheetah-v3: Clipped score of A2C and PPO with and without consistent dropout probabilities 0/0.1/0.25/0.5. Curves are averages of three independent training runs.

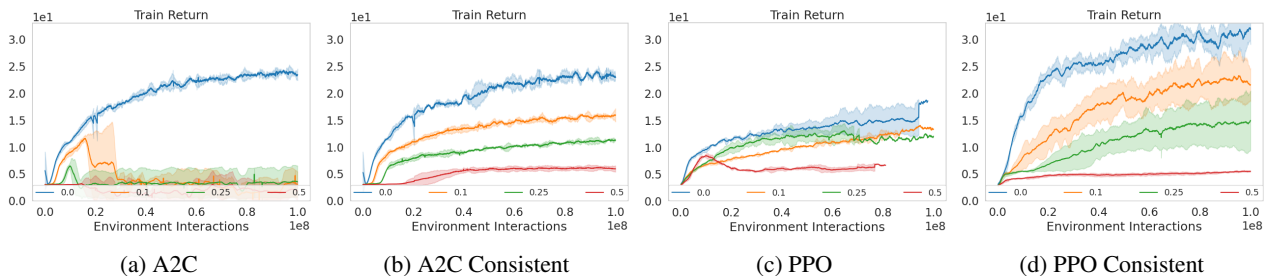


Figure 6. Atari-Beamrider: Clipped score of A2C and PPO with inconsistent and consistent dropout probabilities 0/0.1/0.25/0.5. Curves reflect averages of three independent training runs.

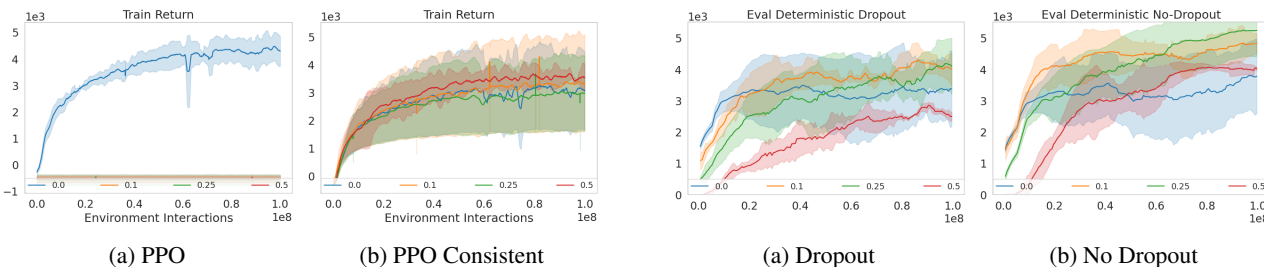


Figure 7. GPT Training: PPO training of GPT models on HalfCheetah-v3. With any level of inconsistent dropout all PPO models are unable to learn. Consistent dropout stabilizes training for all dropout probabilities.

score for the $p = 0.5$ models. Finally, we find that models trained with inconsistent dropout are largely unaffected by enabling or disabling dropout at evaluation time. Further evaluation results may be found in Appendix C.

8. Limitations

This study pertains only to on-policy policy gradient methods. Other types of reinforcement learning algorithms such as off-policy and model-based reinforcement learning are affected by dropout in different ways, which are beyond the scope of this paper.

Having stabilized dropout for policy gradient algorithms, our findings raise the larger question of whether dropout

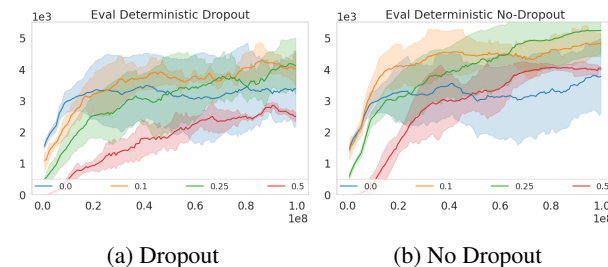


Figure 8. Evaluating with Dropout: Evaluation performance of Consistent PPO on Half-Cheetah-v3 with dropout enabled and disabled for dropout probabilities 0/0.1/0.25/0.5. Similar to supervised learning, disabling dropout at evaluation time increases evaluation performance, particularly with a dropout of 0.5. Curves reflect evaluations performed on models from three independent training runs.

aids generalization to unseen tasks or novel variations of training environments. Related work (Cobbe et al., 2018; Farebrother et al., 2018) has found beneficial generalization effects from small amounts of dropout, and its common use in supervised settings suggests that dropout may aid generalization especially when training overparameterized networks. However, we expect that thoroughly exploring how dropout contributes to generalization in sequential decision settings is a substantial undertaking, one that lies beyond the scope of this work.

9. Conclusions

We demonstrate that naïve application of dropout to policy gradient reinforcement learning results in instability due to the mismatch between the dropout masks that are applied during rollouts and those used during updates. We address this instability through consistent dropout, a simple approach for saving and reapplying the same dropout masks during rollouts and updates. We demonstrate that this solution is both theoretically sound and empirically stable on a variety of continuous and discrete actions environments. Additionally, we show that this technique scales to enable stable online training of transformer models such as GPT. Given the complete lack of support for dropout in open-source reinforcement learning frameworks, we hope this work will pave the way for a re-evaluation of this time-tested technique.

References

- Berner, C., Brockman, G., Chan, B., Cheung, V., Debiak, P., Dennison, C., Farhi, D., Fischer, Q., Hashme, S., Hesse, C., Józefowicz, R., Gray, S., Olsson, C., Pachocki, J., Petrov, M., de Oliveira Pinto, H. P., Raiman, J., Salimans, T., Schlatter, J., Schneider, J., Sidor, S., Sutskever, I., Tang, J., Wolski, F., and Zhang, S. Dota 2 with large scale deep reinforcement learning. *CoRR*, abs/1912.06680, 2019. URL <http://arxiv.org/abs/1912.06680>.
- Castro, P. S., Moitra, S., Gelada, C., Kumar, S., and Bellemare, M. G. Dopamine: A Research Framework for Deep Reinforcement Learning. 2018. URL <http://arxiv.org/abs/1812.06110>.
- Chen, L., Lu, K., Rajeswaran, A., Lee, K., Grover, A., Laskin, M., Abbeel, P., Srinivas, A., and Mordatch, I. Decision transformer: Reinforcement learning via sequence modeling. *CoRR*, abs/2106.01345, 2021. URL <https://arxiv.org/abs/2106.01345>.
- Cobbe, K., Klimov, O., Hesse, C., Kim, T., and Schulman, J. Quantifying generalization in reinforcement learning. *CoRR*, abs/1812.02341, 2018. URL <http://arxiv.org/abs/1812.02341>.
- Cobbe, K., Hesse, C., Hilton, J., and Schulman, J. Leveraging procedural generation to benchmark reinforcement learning. *arXiv preprint arXiv:1912.01588*, 2019.
- Dhariwal, P., Hesse, C., Klimov, O., Nichol, A., Plappert, M., Radford, A., Schulman, J., Sidor, S., Wu, Y., and Zhokhov, P. OpenAI Baselines. <https://github.com/openai/baselines>, 2017.
- Farebrother, J., Machado, M. C., and Bowling, M. Generalization and regularization in DQN. *CoRR*, abs/1810.00123, 2018. URL <http://arxiv.org/abs/1810.00123>.
- Janner, M., Li, Q., and Levine, S. Offline reinforcement learning as one big sequence modeling problem. *Advances in Neural Information Processing Systems*, 34, 2021.
- Liang, E., Liaw, R., Nishihara, R., Moritz, P., Fox, R., Gonzalez, J., Goldberg, K., and Stoica, I. Ray RL-Lib: A Composable and Scalable Reinforcement Learning Library. *CoRR*, abs/1712.09381, 2017. URL <http://arxiv.org/abs/1712.09381>.
- Loynd, R., Fernandez, R., Celikyilmaz, A., Swaminathan, A., and Hausknecht, M. Working memory graphs. In *International Conference on Machine Learning*, pp. 6404–6414. PMLR, 2020.
- Mnih, V., Kavukcuoglu, K., Silver, D., Rusu, A. A., Veness, J., Bellemare, M. G., Graves, A., Riedmiller, M., Fidjeland, A. K., Ostrovski, G., Petersen, S., Beattie, C., Sadik, A., Antonoglou, I., King, H., Kumaran, D., Wierstra, D., Legg, S., and Hassabis, D. Human-level control through deep reinforcement learning. *Nature*, 518 (7540):529–533, February 2015. ISSN 00280836. URL <http://dx.doi.org/10.1038/nature14236>.
- Parisotto, E., Song, H. F., Rae, J. W., Pascanu, R., Gülçehre, Ç., Jayakumar, S. M., Jaderberg, M., Kaufman, R. L., Clark, A., Noury, S., Botvinick, M. M., Heess, N., and Hadsell, R. Stabilizing transformers for reinforcement learning. *CoRR*, abs/1910.06764, 2019. URL <http://arxiv.org/abs/1910.06764>.
- Radford, A., Wu, J., Child, R., Luan, D., Amodei, D., and Sutskever, I. Language models are unsupervised multitask learners. 2019.
- Raffin, A., Hill, A., Ernestus, M., Gleave, A., Kanervisto, A., and Dormann, N. Stable-Baselines3. <https://github.com/DLR-RM/stable-baselines3>, 2019.
- Schulman, J., Heess, N., Weber, T., and Abbeel, P. Gradient estimation using stochastic computation graphs. In *Advances in Neural Information Processing Systems*, 2015.
- Schulman, J., Moritz, P., Levine, S., Jordan, M., and Abbeel, P. High-dimensional continuous control using generalized advantage estimation. In *International Conference on Learning Representations*, 2016.
- Schulman, J., Wolski, F., Dhariwal, P., Radford, A., and Klimov, O. Proximal policy optimization algorithms. *CoRR*, abs/1707.06347, 2017. URL <http://arxiv.org/abs/1707.06347>.

- Silver, D., Huang, A., Maddison, C. J., Guez, A., Sifre, L., van den Driessche, G., Schrittwieser, J., Antonoglou, I., Panneershelvam, V., Lanctot, M., Dieleman, S., Grewe, D., Nham, J., Kalchbrenner, N., Sutskever, I., Lillicrap, T., Leach, M., Kavukcuoglu, K., Graepel, T., and Hassabis, D. Mastering the game of Go with deep neural networks and tree search. *Nature*, 529(7587):484–489, Jan 2016. ISSN 0028-0836. doi: 10.1038/nature16961.
- Srivastava, N., Hinton, G., Krizhevsky, A., Sutskever, I., and Salakhutdinov, R. Dropout: A simple way to prevent neural networks from overfitting. *Journal of Machine Learning Research*, 15(56):1929–1958, 2014. URL <http://jmlr.org/papers/v15/srivastava14a.html>.
- Stooke, A. and Abbeel, P. rlpyt: A Research Code Base for Deep Reinforcement Learning in PyTorch. *CoRR*, abs/1909.01500, 2019. URL <http://arxiv.org/abs/1909.01500>.
- Sutton, R. S., McAllester, D. A., Singh, S. P., and Mansour, Y. Policy gradient methods for reinforcement learning with function approximation. In *Advances in Neural Information Processing Systems*, pp. 1057–1063, 2000.
- Vaswani, A., Shazeer, N., Parmar, N., Uszkoreit, J., Jones, L., Gomez, A. N., Kaiser, L. u., and Polosukhin, I. Attention is all you need. In *Advances in Neural Information Processing Systems*, volume 30. Curran Associates, Inc., 2017. URL <https://proceedings.neurips.cc/paper/2017/file/3f5ee243547dee91fbd053c1c4a845aa-Paper.pdf>.
- Vinyals, O., Babuschkin, I., Chung, J., Mathieu, M., Jaderberg, M., Czarnecki, W., Dudzik, A., Huang, A., Georgiev, P., Powell, R., Ewalds, T., Horgan, D., Kroiss, M., Danihelka, I., Agapiou, J., Oh, J., Dalibard, V., Choi, D., Sifre, L., Sulsky, Y., Vezhnevets, S., Molloy, J., Cai, T., Budden, D., Paine, T., Gulcehre, C., Wang, Z., Pfaff, T., Pohlen, T., Yogatama, D., Cohen, J., McKinney, K., Smith, O., Schaul, T., Lillicrap, T., Apps, C., Kavukcuoglu, K., Hassabis, D., and Silver, D. AlphaStar: Mastering the Real-Time Strategy Game StarCraft II. <https://deepmind.com/blog/alphastar-mastering-real-time-strategy-game-starcraft-ii/>, 2019.
- Weng, J., Zhang, M., Yan, D., Su, H., and Zhu, J. Tianshou. <https://github.com/thu-ml/tianshou>, 2020.

A. Hyperparameters

Table 3. **Hyperparameters:** Networks consisted of 3-layer MLPs with ReLU nonlinearities. Dropout was applied between each layer of the network. Note that PPO Consistent uses a target-KL early stopping condition to terminate updates when the KL divergence passes a threshold. We attempted to run standard PPO with the same parameter but found that it would trigger early termination due to the large KL divergences caused by inconsistent dropout masks. Thus, the best performance for standard PPO was with the target-KL disabled.

VARIANT	HYPERPARAMETER	MUJoCo	ATARI
A2C & A2C CONSISTENT	MAX STEPS	1E8	1E8
	WORKERS	16	16
	STEPS PER EPOCH	80	5
	LEARNING RATE	7E-4	1E-4
	CRITIC LR	7E-4	-
	ENTROPY COEFFICIENT	0.01	0.01
	DISCOUNT FACTOR	0.99	0.99
	GAE-LAMBDA	0.95	0.95
	HIDDEN SIZE	64	512
	GRADIENT NORM CLIP	0.5	0.5
	RMS PROP EPSILON	3E-6	3E-6
	ADVANTAGE NORMALIZATION	1	0
	PPO	MAX STEPS	1E8
WORKERS		16	16
LEARNING RATE		3E-4	1E-4
STEPS PER EPOCH		4096	4096
GRADIENT STEPS PER UPDATE		16	16
BATCH SIZE		64	64
HIDDEN SIZE		64	512
VALUE COEFFICIENT		0.5	0.5
ENTROPY COEFFICIENT		0.01	0
GRADIENT NORM CLIP		0.5	0.5
DISCOUNT FACTOR		0.99	0.99
GAE-LAMBDA		0.97	0.95
CLIP RATIO		0.2	0.2
TARGET KL		-	-
PPO CONSISTENT	MAX STEPS	1E8	1E8
	WORKERS	16	16
	LEARNING RATE	3E-4	1E-4
	STEPS PER EPOCH	4096	4096
	GRADIENT STEPS PER UPDATE	16	16
	BATCH SIZE	64	64
	HIDDEN SIZE	64	512
	VALUE COEFFICIENT	0.5	0.5
	ENTROPY COEFFICIENT	0.01	0
	GRADIENT NORM CLIP	0.5	0.5
	DISCOUNT FACTOR	0.99	0.99
	GAE-LAMBDA	0.97	0.95
	CLIP RATIO	0.2	0.2
	TARGET KL	0.01	0.01
GPT & GPT CONSISTENT	MAX STEPS	1E8	
	WORKERS	16	
	LEARNING RATE	3E-4	
	CRITIC LEARNING RATE	7E-4	
	STEPS PER EPOCH	1024	
	GRADIENT STEPS PER UPDATE	128	
	BATCH SIZE	64	
	HIDDEN SIZE	64	
	ENTROPY COEFFICIENT	0.01	
	GRADIENT NORM CLIP	0.5	
	DISCOUNT FACTOR	0.99	
	GAE-LAMBDA	0.97	
	CLIP RATIO	0.2	
	TARGET KL	0.01	
BLOCK SIZE	8		
NUMBER OF LAYERS	4		
NUMBER OF HEADS	4		

B. RL Framework Testing

The following tables show results from testing *inconsistent dropout* on three open-source reinforcement learning frameworks. This was accomplished by adding dropout layers to the policy networks and running the A2C and PPO on the HalfCheetah-v3 environment using the hyperparameters suggested by the respective codebase. In all the following tables, where ReLU was not used, Tanh was applied.

Table 4. Tianshou (version 0.4.2) on HalfCheetah-v3: For A2C, ReLU activation seems to be the biggest causative factor of instability, while Tanh is a stabilizer. ActionClipping can also help stabilize when dropout levels are moderate. Reward normalization may have a slightly helpful effect, but less than other factors. PPO even with moderate levels of dropout demonstrated broad instability: PPO[†] indicates early termination of the experiment due to instabilities resulting in NaN values.

ALG	DROPOUT	REWNORM?	ACTCLIP?	RELU?	BEST	FINAL
A2C	0	✓	✓	✗	1556	1542
A2C	0	✓	✓	✓	2949	2927
A2C	0.1	✗	✓	✗	3192	2969
A2C	0.1	✗	✓	✓	3085	2693
A2C	0.1	✗	✗	✗	3593	3357
A2C	0.1	✗	✗	✓	1628	-3e7
A2C	0.1	✓	✓	✗	1193	1152
A2C	0.1	✓	✓	✓	537	573
A2C	0.1	✓	✗	✗	3066	2900
A2C	0.1	✓	✗	✓	3204	-1.2e8
A2C	0.25	✗	✓	✗	1049	977
A2C	0.25	✗	✓	✓	171	-13
A2C	0.25	✗	✗	✗	1065	-3.4e7
A2C	0.25	✗	✗	✓	-146	-3.9e9
A2C	0.25	✓	✓	✗	1141	1139
A2C	0.25	✓	✓	✓	1137	1048
A2C	0.25	✓	✗	✗	3872	3313
A2C	0.25	✓	✗	✓	260	-2.1e9
PPO	0	✓	✓	✗	7472	5645
PPO	0	✓	✓	✓	8743	7890
PPO [†]	0.1	✗	✓	✗	1708	-335
PPO [†]	0.1	✗	✓	✓	1548	463
PPO [†]	0.1	✗	✗	✗	2267	1162
PPO [†]	0.1	✗	✗	✓	1372	1050
PPO [†]	0.1	✓	✓	✗	2238	1813
PPO [†]	0.1	✓	✓	✓	408	42
PPO [†]	0.1	✓	✗	✗	2268	1870
PPO [†]	0.1	✓	✗	✓	1007	-55
PPO [†]	0.25	✗	✓	✗	1001	881
PPO [†]	0.25	✗	✓	✓	279	153
PPO [†]	0.25	✗	✗	✗	1270	1006
PPO [†]	0.25	✗	✗	✓	614	246
PPO [†]	0.25	✓	✓	✗	1292	1167
PPO [†]	0.25	✓	✓	✓	705	-123
PPO [†]	0.25	✓	✗	✗	348	1321
PPO [†]	0.25	✓	✗	✓	348	-160

Consistent Dropout

Table 5. Stable-Baselines3 (version 1.2.0a0) on HalfCheetah-v3. Policy loss is shown in to provide an intuition on about the stability of the training process. Very high policy losses correlate to high-magnitude $\log \pi(a|s)$ values, a symptom of unstable dynamics induced by inconsistent dropout.

ALG	DROPOUT	RELU?	ORTHO INIT?	FINAL	POLICY LOSS
A2C	0	✗	✗	974	2.5
A2C	0	✗	✓	688	-1.1
A2C	0	✓	✗	526	8
A2C	0	✓	✓	1954	-5.4
A2C	0.1	✗	✗	1003	-12.1
A2C	0.1	✗	✓	650	-8.8
A2C	0.1	✓	✗	1639	8.8e3
A2C	0.1	✓	✓	-40	-242
A2C	0.25	✗	✗	1325	26
A2C	0.25	✗	✓	499	25
A2C	0.25	✓	✗	1497	-2.9e5
A2C	0.25	✓	✓	950	-2.7e5
A2C	0.5	✗	✗	116	1e3
A2C	0.5	✗	✓	639	-7.2e3
A2C	0.5	✓	✗	1527	1.7e8
A2C	0.5	✓	✓	1083	-7.8e8
PPO	0	✗	✗	2238	-0.007
PPO	0	✗	✓	3211	-0.001
PPO	0	✓	✗	1232	-0.0006
PPO	0	✓	✓	1277	-0.001
PPO	0.1	✗	✗	1963	0.04
PPO	0.1	✗	✓	1256	0.05
PPO	0.1	✓	✗	1830	0.04
PPO	0.1	✓	✓	2463	0.04
PPO	0.25	✗	✗	1468	0.04
PPO	0.25	✗	✓	1383	0.04
PPO	0.25	✓	✗	2217	0.05
PPO	0.25	✓	✓	1825	0.05
PPO	0.5	✗	✗	1331	0.06
PPO	0.5	✗	✓	1328	0.06
PPO	0.5	✓	✗	904	0.06
PPO	0.5	✓	✓	993	0.05

Table 6. RLLib (version 1.8.0) on HalfCheetah-v3. Dagger denotes training became numerically unstable and produced errors. For these runs, we report the final performance level before the error.

ALG	DROPOUT	RELU?	FINAL
A2C	0	✗	712
A2C	0	✓	747
A2C	0.1	✗	-393
A2C [†]	0.1	✓	-439
A2C [†]	0.25	✗	-253
A2C [†]	0.25	✓	-594
A2C [†]	0.5	✗	-643
A2C [†]	0.5	✓	-596
PPO	0	✗	2044
PPO	0	✓	5390
PPO	0.1	✗	909
PPO [†]	0.1	✓	-109
PPO	0.25	✗	383
PPO [†]	0.25	✓	-238
PPO	0.5	✗	867
PPO	0.5	✓	1517

C. Full MuJoCo Results

Hyperparameters were tuned on Half-Cheetah-v3 then deployed without further modification on Hopper-v3 and Walker2d-v3.

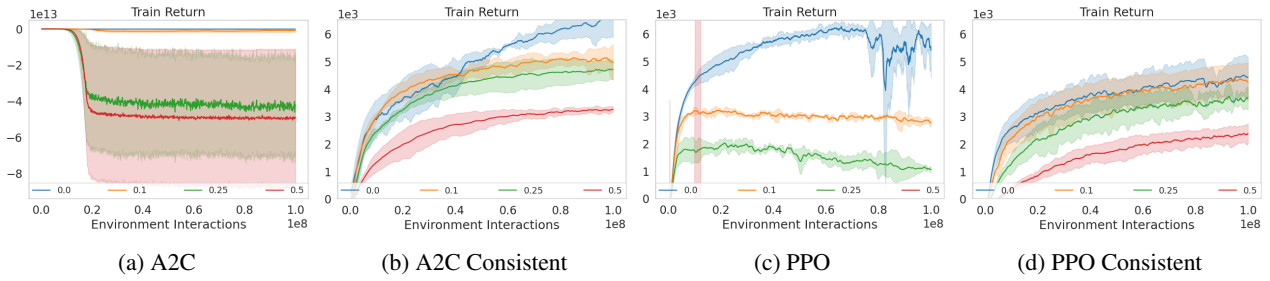


Figure 9. **Half-Cheetah-v3**: Training performance of various models on MuJoCo Half-Cheetah-v3. Curves are averages of three independent training runs.

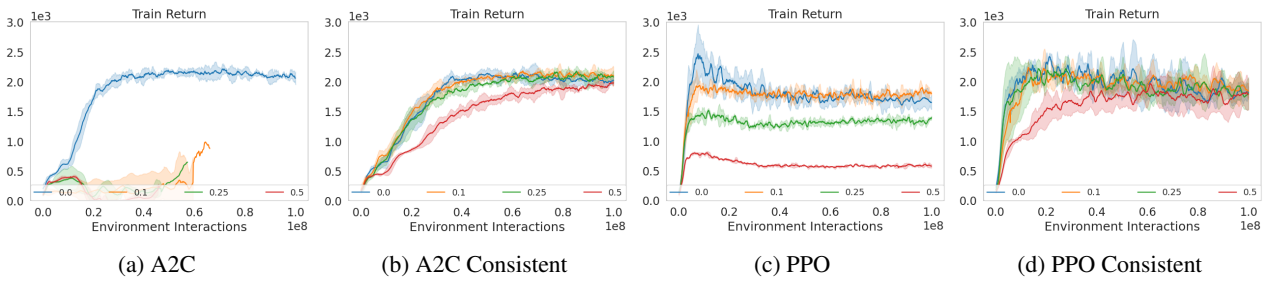


Figure 10. **Hopper-v3**: Training performance of various models on MuJoCo Hopper-v3. Curves are averages of three independent training runs.

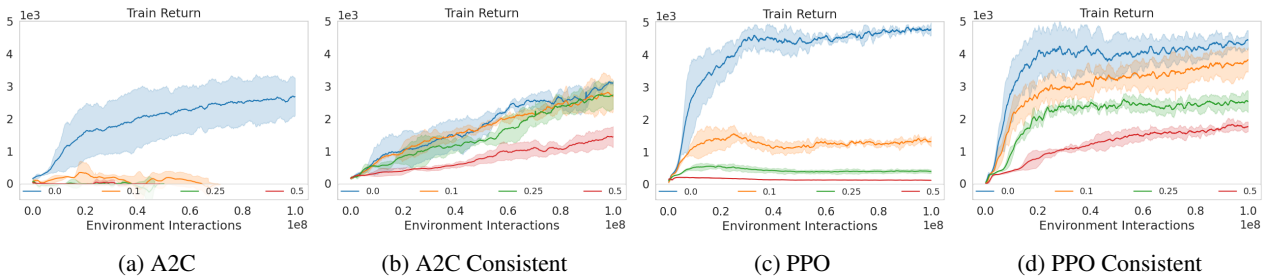


Figure 11. **Walker2d-v3**: Training performance of various models on MuJoCo Walker2d-v3. Curves are averages of three independent training runs.

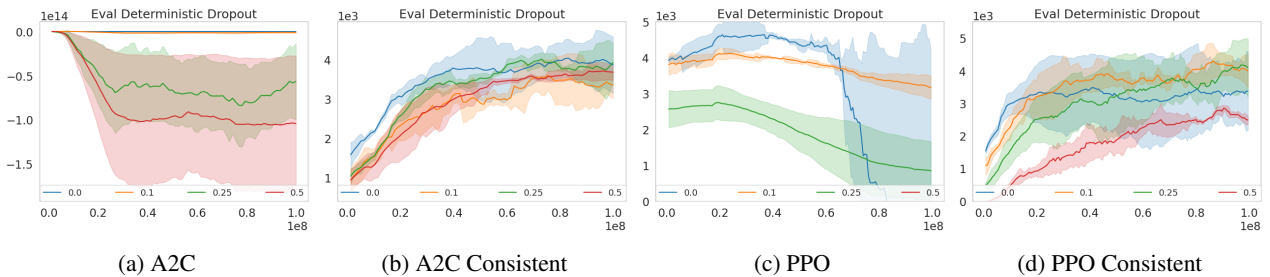


Figure 12. **Half-Cheetah-v3 Deterministic Evaluation with Dropout**: Curves are averages of three independent training runs.

Consistent Dropout

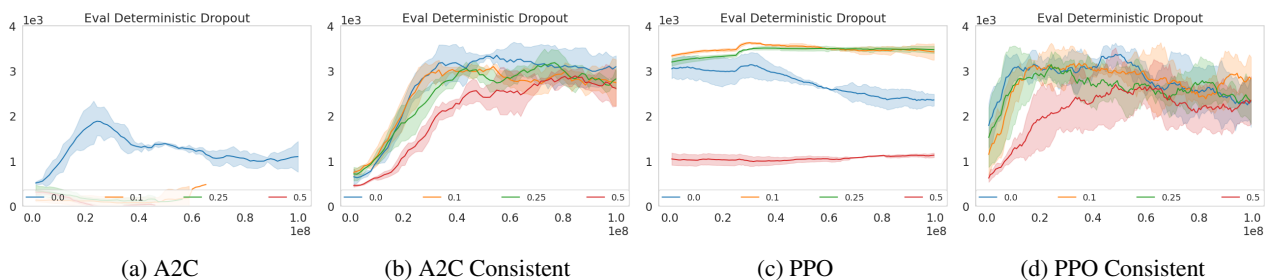


Figure 13. Hopper-v3 Deterministic Evaluation with Dropout: Curves are averages of three independent training runs.

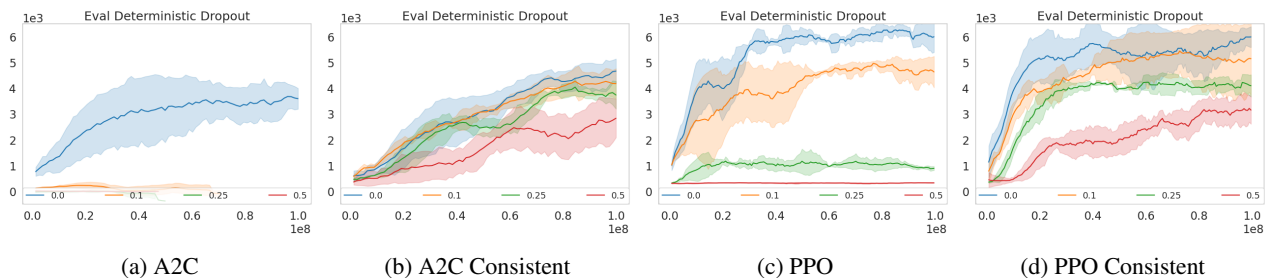


Figure 14. Walker2d-v3 Deterministic Evaluation with Dropout: Curves are averages of three independent training runs.

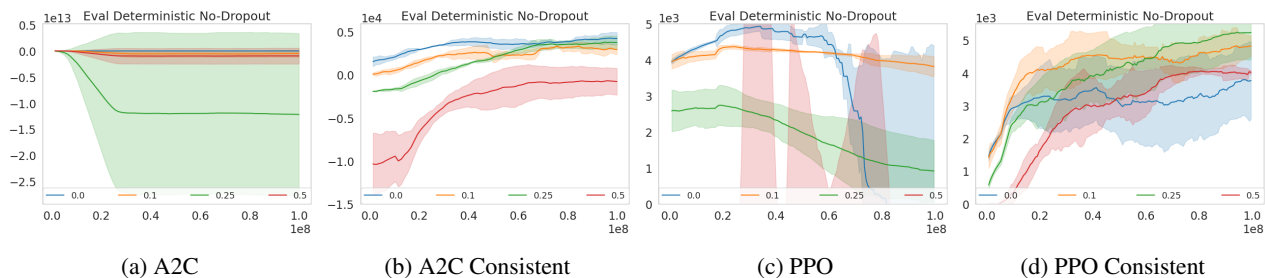


Figure 15. Half-Cheetah-v3 Deterministic Evaluation No-Dropout: Curves are averages of three independent training runs.

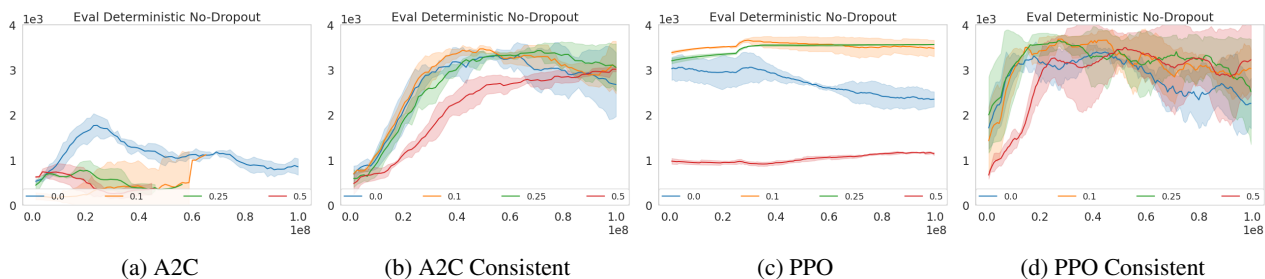


Figure 16. Hopper-v3 Deterministic Evaluation No-Dropout: Curves are averages of three independent training runs.

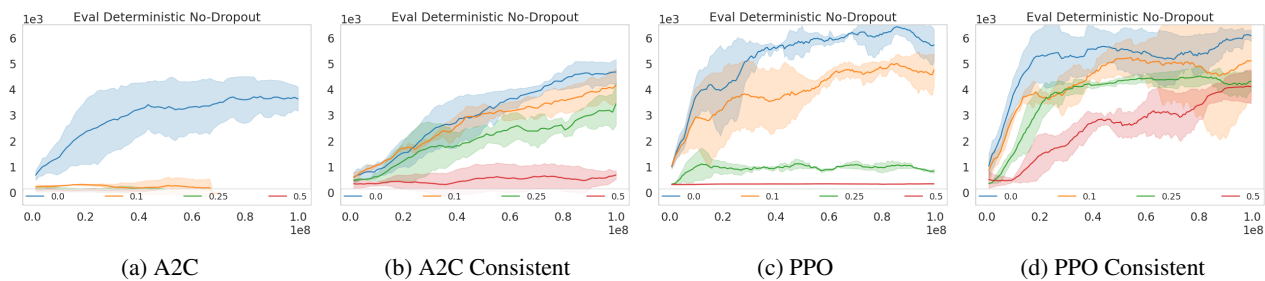


Figure 17. Walker2d-v3 Deterministic Evaluation No-Dropout: Curves are averages of three independent training runs.

D. Full Atari Results

Hyperparameters were tuned for Beamrider then deployed without further modification on Breakout and Seaquest. The lower performance from PPO without dropout versus PPO Consistent without dropout is due to the lack of target-KL early stopping threshold for PPO. If this threshold is not disabled, PPO, due to inconsistent dropout, fails to perform any policy updates and makes no learning progress.

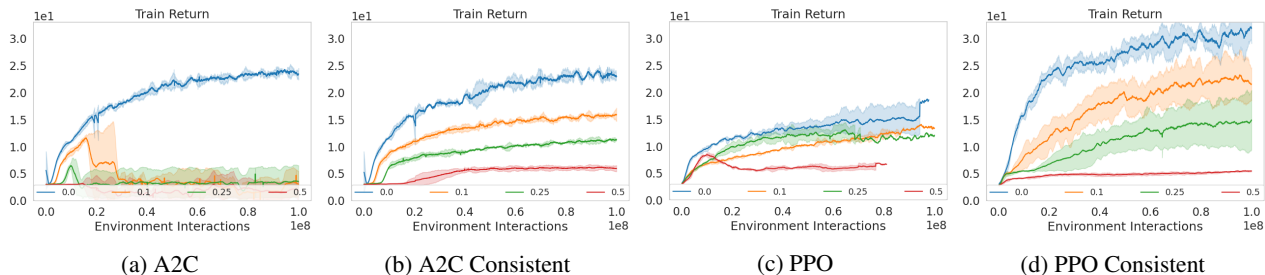


Figure 18. **Beamrider**: Training performance of various models on Atari Beamrider. Curves are averages of three independent training runs.

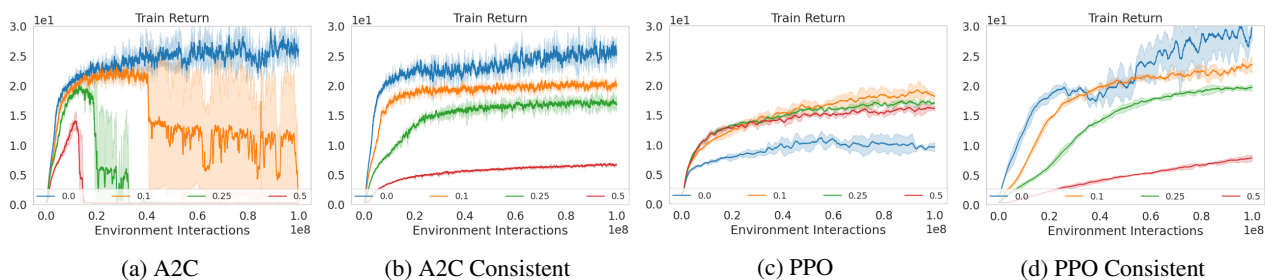


Figure 19. **Breakout**: Training performance of various models on Atari Breakout. Curves are averages of three independent training runs.

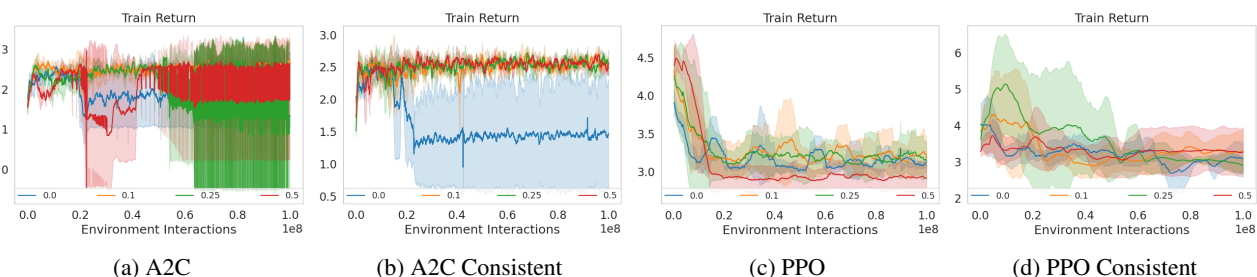


Figure 20. **Seaquest**: Training performance of various models on Atari Seaquest. Curves are averages of three independent training runs. Poor performance from all algorithms indicates hyperparameters which were tuned for Beamrider are suboptimal for Seaquest.

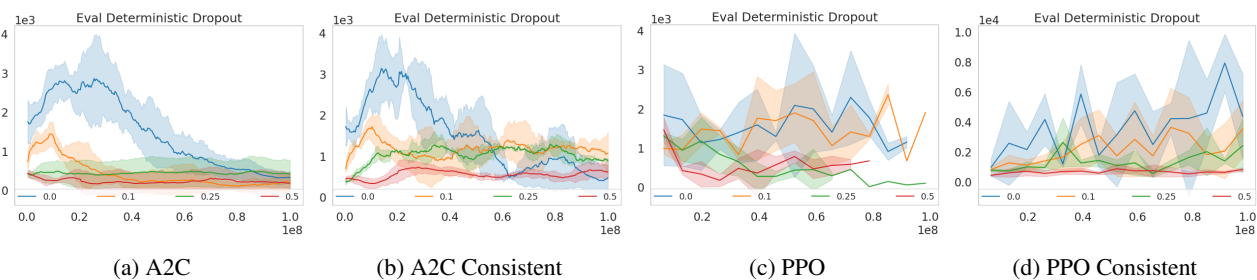


Figure 21. **Beamrider Deterministic Evaluation with Dropout**: Curves are averages of three independent training runs.

Consistent Dropout

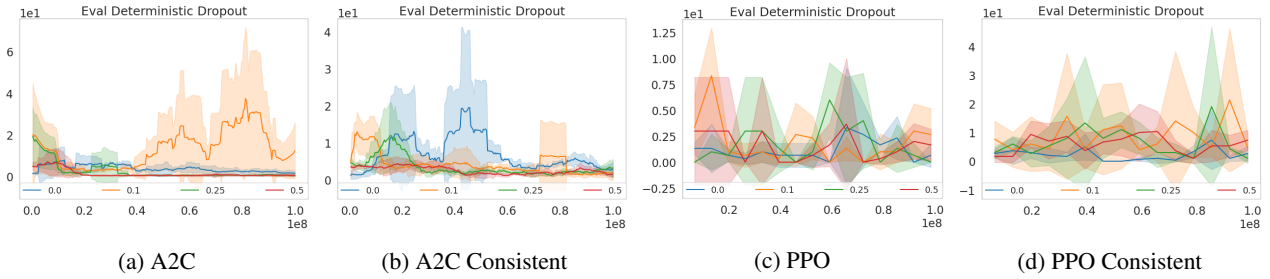


Figure 22. Breakout Deterministic Evaluation with Dropout: Curves are averages of three independent training runs.

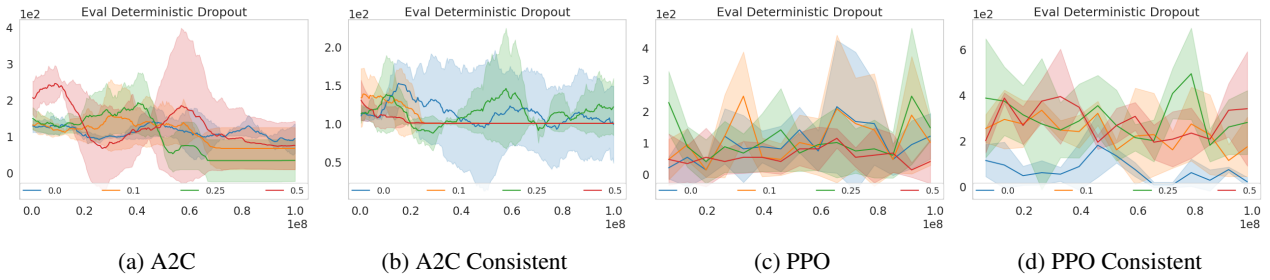


Figure 23. Seaquest Deterministic Evaluation with Dropout: Curves are averages of three independent training runs.

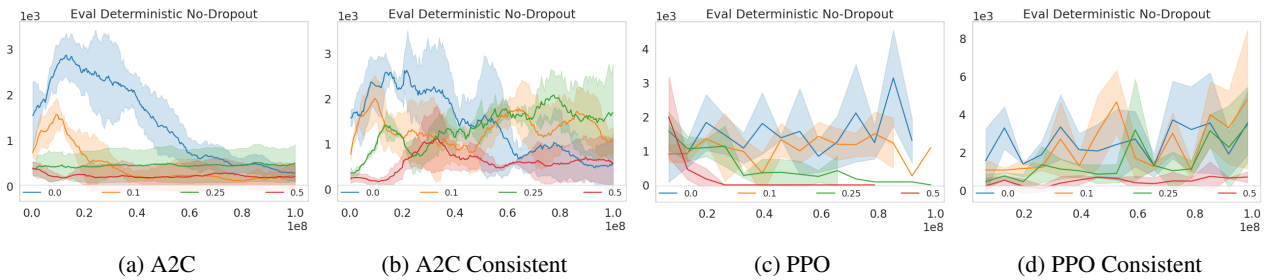


Figure 24. Beamrider Deterministic Evaluation with No-Dropout: Curves are averages of three independent training runs.

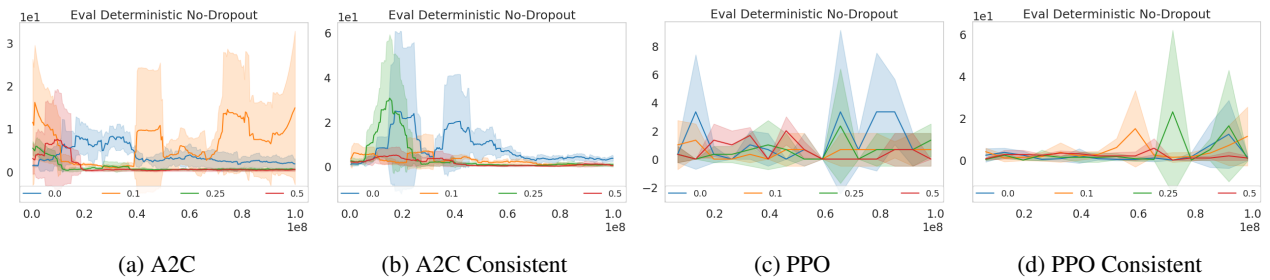


Figure 25. Breakout Deterministic Evaluation with No-Dropout: Curves are averages of three independent training runs.

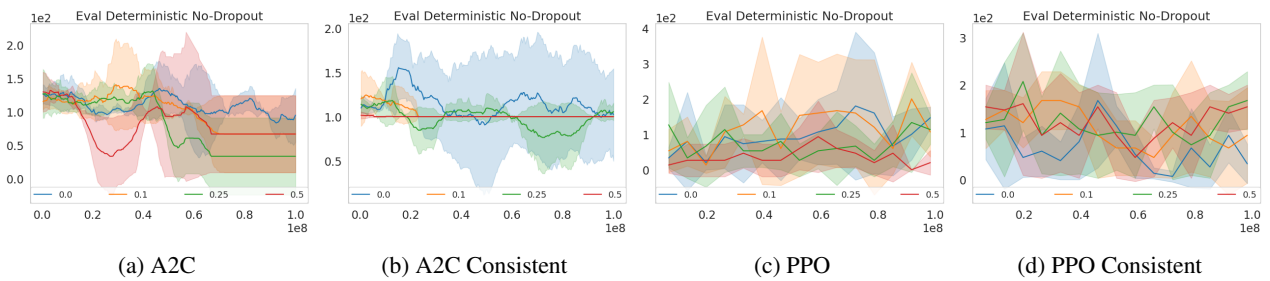


Figure 26. Seaquest Deterministic Evaluation with No-Dropout: Curves are averages of three independent training runs.